Hyperoxaluria Requires TNF Receptors to Initiate Crystal Adhesion and Kidney Stone Disease

Shrikant R. Mulay,* Jonathan N. Eberhard,* Jyaysi Desai,* Julian A. Marschner,*
Santhosh V.R. Kumar,* Marc Weidenbusch,* Melissa Grigorescu,* Maciej Lech,* Nuru Eltrich,*
Lisa Müller,[†] Wolfgang Hans,[‡] Martin Hrabĕ de Angelis,[‡§ǁ] Volker Vielhauer,* Bernd Hoppe,[¶]
John Asplin,** Nicolai Burzlaff,[†] Martin Herrmann,[††] Andrew Evan,[‡‡] and
Hans-Joachim Anders*

*Nephrologisches Zentrum, Medizinische Klinik und Poliklinik IV, Klinikum der Universität München, Munich, Germany;
[†]Department of Chemistry and Pharmacy and Interdisciplinary Center for Molecular Materials, Inorganic Chemistry and
Interdisciplinary Center for Molecular Materials, Friedrich-Alexander-Universität Erlangen-Nürnberg, Erlangen, Germany;
[‡]German Mouse Clinic, Institute of Experimental Genetics, Helmholtz-Zentrum München, Neuherberg, Germany;
[§]Institute of Molecular Animal Breeding and Biotechnology, Gene Center, Ludwig-Maximilians University München,
Munich, Germany; [ǁ]German Center for Diabetes Research, Neuherberg, Germany; [¶]Department of Pediatrics, University
Medical Center, Bonn, Germany; **Litholink Corporation, Laboratory Corporation of America Holdings, Chicago, Illinois;
[††]Department for Internal Medicine 3, University Hospital Erlangen, Institute for Clinical Immunology, Erlangen,
Germany; and [‡‡]Department of Anatomy and Cell Biology, Indiana University School of Medicine, Indianapolis, Indiana

ABSTRACT

Intrarenal crystals trigger inflammation and renal cell necroptosis, processes that involve TNF receptor (TNFR) signaling. Here, we tested the hypothesis that TNFRs also have a direct role in tubular crystal deposition and progression of hyperoxaluria-related CKD. Immunohistochemical analysis revealed upregulated tubular expression of TNFR1 and TNFR2 in human and murine kidneys with calcium oxalate (CaOx) nephrocalcinosis-related CKD compared with controls. Western blot and mRNA expression analyses in mice yielded consistent data. When fed an oxalate-rich diet, wild-type mice developed progressive CKD, whereas *Tnfr1-*, *Tnfr2-*, and *Tnfr1/2-* deficient mice did not. Despite identical levels of hyperoxaluria, *Tnfr1-*, *Tnfr2-*, and *Tnfr1/2*-deficient mice also lacked the intrarenal CaOx deposition and tubular damage observed in wild-type mice. Inhibition of TNFR signaling prevented the induced expression of the crystal adhesion molecules, CD44 and annexin II, in tubular epithelial cells *in vitro* and *in vivo*, and treatment with the small molecule TNFR inhibitor R-7050 partially protected hyperoxaluric mice from nephrocalcinosis and CKD. We conclude that TNFR signaling is essential for CaOx crystal adhesion to the luminal membrane of renal tubules as a fundamental initiating mechanism of oxalate nephropathy. Furthermore, therapeutic blockade of TNFR might delay progressive forms of nephrocalcinosis in oxalate nephropathy, such as primary hyperoxaluria.

Kidney stone disease, *i.e.*, nephro-/urolithiasis, affects around 12% of men and 5% of women during their lifetime.[1] In contrast, nephrocalcinosis is usually asymptomatic but can lead to progressive nephron loss and CKD.[1,2] Calcium oxalate (CaOx) stones account for the vast majority of calculi in stone formers, and complicate primary and secondary forms of hyperoxaluria.[1] Idiopathic CaOx stone formers are characterized by hypercalciuria, interstitial calcium phosphate deposits (Randall plaque) at the papillary tip, and attached CaOx stones.[3] The traditional pathogenic concepts of nephrolithiasis are based on urine supersaturation of minerals or the lack of sufficient crystallization inhibitors.[4–6] Intratubular crystals adhere to the luminal membrane of tubular epithelial cells *via* a group of adhesion molecules.[7–14] Adherent crystals form a nidus for intratubular crystal plug formation, leading to tubule obstruction and nephron atrophy.[2,15,16] In primary hyperoxaluria, nephrocalcinosis-related progressive nephron loss can progress to ESRD.[2,15,17] NLRP3 inflammasome-mediated intrarenal inflammation contributes to acute and chronic oxalosis in
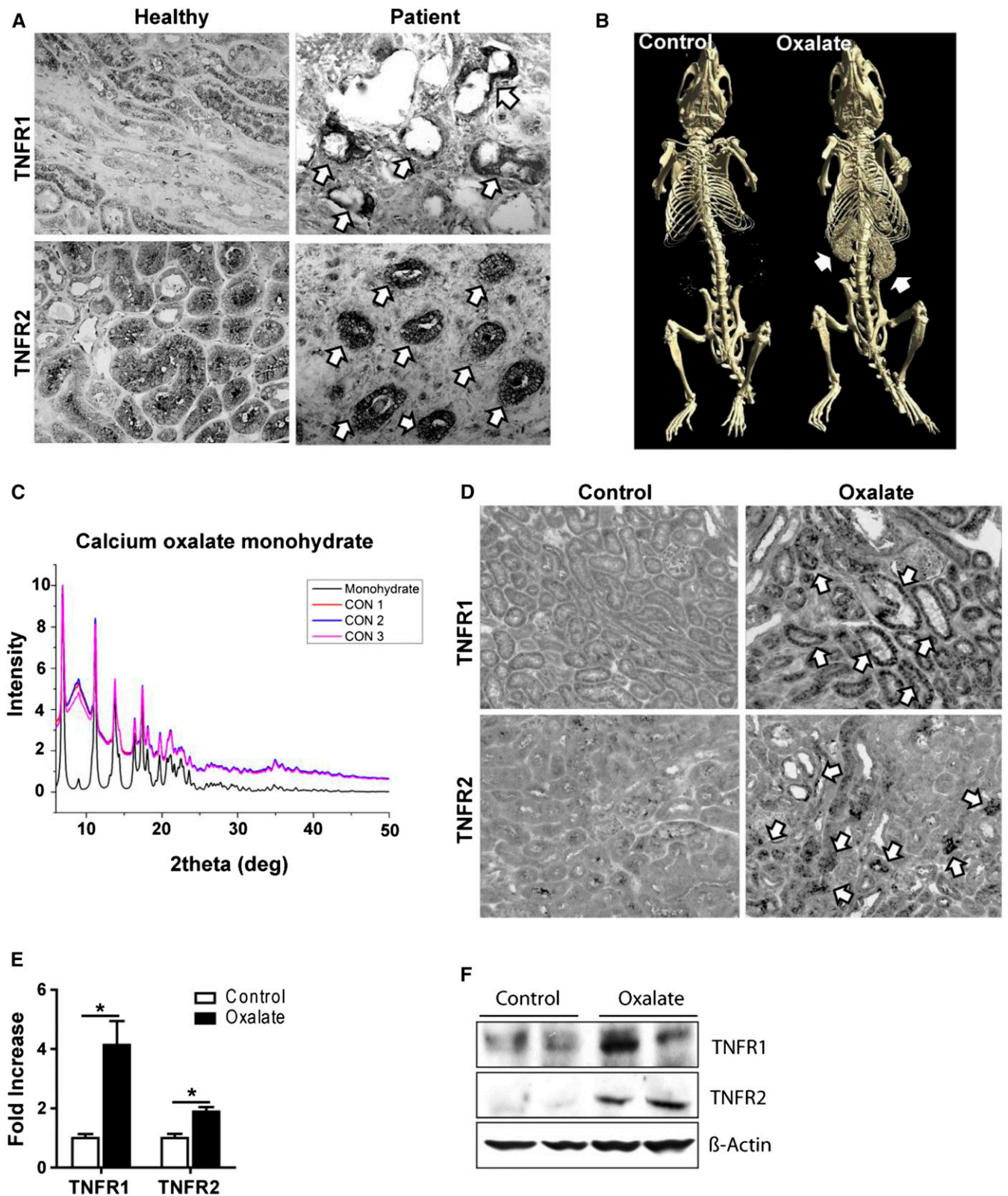
Figure 1. Humans and mice with hyperoxaluria express TNFR1 and TNFR2 in tubular epithelial cells. (A) Immunostaining for TNFR1 and TNFR2 in kidney tissue obtained from healthy donors, as well as from patients with hyperoxaluria-related CKD. Arrows indicate positivity for TNFR1 and TNFR2, respectively. (B–F) C57BL/6 male mice were fed either high control or high oxalate diet for 14 days. (B) Diagnostic imaging was conducted using computed tomography. Arrows indicate nephrocalcinosis. (C) The analysis of the mouse kidneys was

mice,[18,19] and proinflammatory cytokines, like TNFα, activate TNF receptor-1 (TNFR1) to trigger tubular epithelial necroptosis in nephrocalcinosis based on CaOx deposition.[20] Here, we investigated the potential contribution of TNFRs to hyperoxaluria-induced nephrocalcinosis and CKD.

To address a potential contribution of TNFRs to CaOx-related CKD, we first studied the expression of TNFR1 and TNFR2 in kidney tissue obtained from healthy donors as well as from patients with hyperoxaluria-related CKD. Immunostaining for TNFR1 and TNFR2 showed strong positivity in renal tubules of diseased kidneys but only weak signals in controls (Figure 1A). Further, immunostaining of kidney sections from mice with CaOx monohydrate-related nephrocalcinosis gave identical results, and was consistent with induction of intrarenal TNFR1 and TNFR2 mRNA and protein expression (Figure 1, B–E, Supplemental Figure 1).

To address a potential functional contribution of TNFR1 and TNFR2 during nephrocalcinosis, we fed mice deficient in *Tnfr1*, *Tnfr2*, and *Tnfr1/2* the same oxalate-rich diet. While wild-type mice developed increased serum markers of impaired excretory renal function, such as elevated BUN and creatinine, this was abrogated in *Tnfr1-*, *Tnfr2-*, and *Tnfr1/2*-deficient mice (Figure 2, A and B). Hyperoxaluria-related CKD in wild-type mice was associated with diffuse tubular atrophy and interstitial fibrosis, together with robust interstitial infiltrates of F4/80+ mononuclear phagocytes and CD3+ T cells (Figure 2, C–E, Supplemental Figure 2A). In contrast, *Tnfr1-*, *Tnfr2-*, and *Tnfr1/2*-deficient mice completely lacked these abnormalities (Figure 2, C–E, Supplemental Figure 2A). These findings are consistent with an entirely normal mRNA expression profile of injury markers and proinflammatory cytokines or histopathologic markers of

renal fibrosis in *Tnfr1-*, *Tnfr2-*, and *Tnfr1/2*-deficient mice. All of these factors showed an increased expression in hyperoxaluric wild-type mice (Supplemental Figure 2, B–D). Computed tomography of oxalate-fed wild-type mice revealed diffuse bilateral nephrocalcinosis, which was absent in all three *Tnfr*-deficient mouse strains (Figure 2G). The more sensitive Pizzolato staining of renal sections confirmed that all three *Tnfr*-deficient mouse strains lacked intrarenal CaOx crystal deposits (Figure 2H). We assessed urinary mineral concentrations to rule out the difference in renal oxalate excretion as a cause of the difference in tubule crystal deposition in *Tnfr1-*, *Tnfr2-*, and *Tnfr1/2*-deficient mice. Mice of all strains developed significant hyperoxaluria upon initiating the oxalate-rich diet. Thus, in the absence of TNFRs, hyperoxaluria no longer causes nephrocalcinosis or CKD.

Hyperoxaluria requires CaOx crystal adhesion to tubular epithelial cells to induce nephrocalcinosis.[9,10,12–14,21] First, we tested for a direct interaction of receptors with crystals by using a soluble fusion protein of either TNFR1 or TNFR2 and human IgG1, which allows quantification of fusion protein binding to crystals with fluorescent anti-human IgG1 secondary reagent. However, no such signal was observed (not shown). To study the possibility of TNFR-mediated induction of the crystal-binding proteins, we isolated tubular epithelial cells of mice of all genotypes, exposed them to CaOx crystals *in vitro*, and quantified CD44 and annexin II mRNA levels 6 hours later. In wild-type cells, CaOx crystals induced the expression of these crystal-binding proteins compared with baseline, a response missing in *Tnfr1/2*-deficient tubular epithelial cells (Figure 3A). To validate this finding *in vivo*, we quantified the expression of CD44 and annexin II in kidneys of hyperoxaluric

mice by RT-PCR and immunostaining. In contrast to wild-type mice, none of the mutant mouse strains showed increased mRNA or protein expression of CD44 and annexin by RT-PCR and immunohistochemistry, respectively (Figure 3, B–D).

If the development of nephrocalcinosis or CKD in conditions of hyperoxaluria requires TNFR-mediated induction of tubular adhesion molecules, then TNFR blockade should be protective. Indeed, TNFR blockade with R-7050 reduced intrarenal mRNA and protein expression of CD44 and annexin II in hyperoxaluric mice (Figure 4, A–C). The TNFR blockade was associated with a protective effect on intrarenal CaOx crystal deposition and reduced levels of BUN, plasma creatinine, and tubular injury (Figure 4, D–F, Supplemental Figure 3A). The mRNA expression levels of markers for tubular injury, intrarenal inflammation, and renal fibrosis (KIM-1, IL-6/CCL5, and collagen-1α1/fibronectin, significantly reduced by treatment with R-7050, respectively) were treated with R-7050 (Supplemental Figure 3, B–D). These results were consistent with a reduced staining in renal sections for F4/80+ macrophages, CD3+ T cells, smooth muscle actin, and Masson Trichrome (Supplemental Figure 3, E–G). We conclude that pharmacologic TNFR inhibition blocks a central pathomechanism of hyperoxaluria-related nephrocalcinosis, and therefore, protects hyperoxaluric mice from CKD progression.

We had speculated on a functional contribution of TNFRs to hyperoxaluria-induced nephrocalcinosis and CKD, since inflammatory pathways and TNFα-mediated renal cell necroptosis were shown to contribute to CaOx crystal-induced kidney pathology.[18–20,22,23] Our data reveal that, during hyperoxaluria, TNFR signaling is required for the development of nephrocalcinosis, and

---

performed by x-ray diffraction. Control (CON): CaOx nephropathy. (D) Immunostaining. Arrows indicate positivity for TNFR1 and TNFR2, respectively. Original magnification ×200. (E) Gene expression for TNFR1 and TNFR2 in kidney tissue obtained from these mice. (F) Protein expression of TNFR1 and TNFR2 was detected using Western blot. β-actin was employed as loading control. Data are means±SEM from six to seven mice in each group. *$P<0.05$ versus the control group.
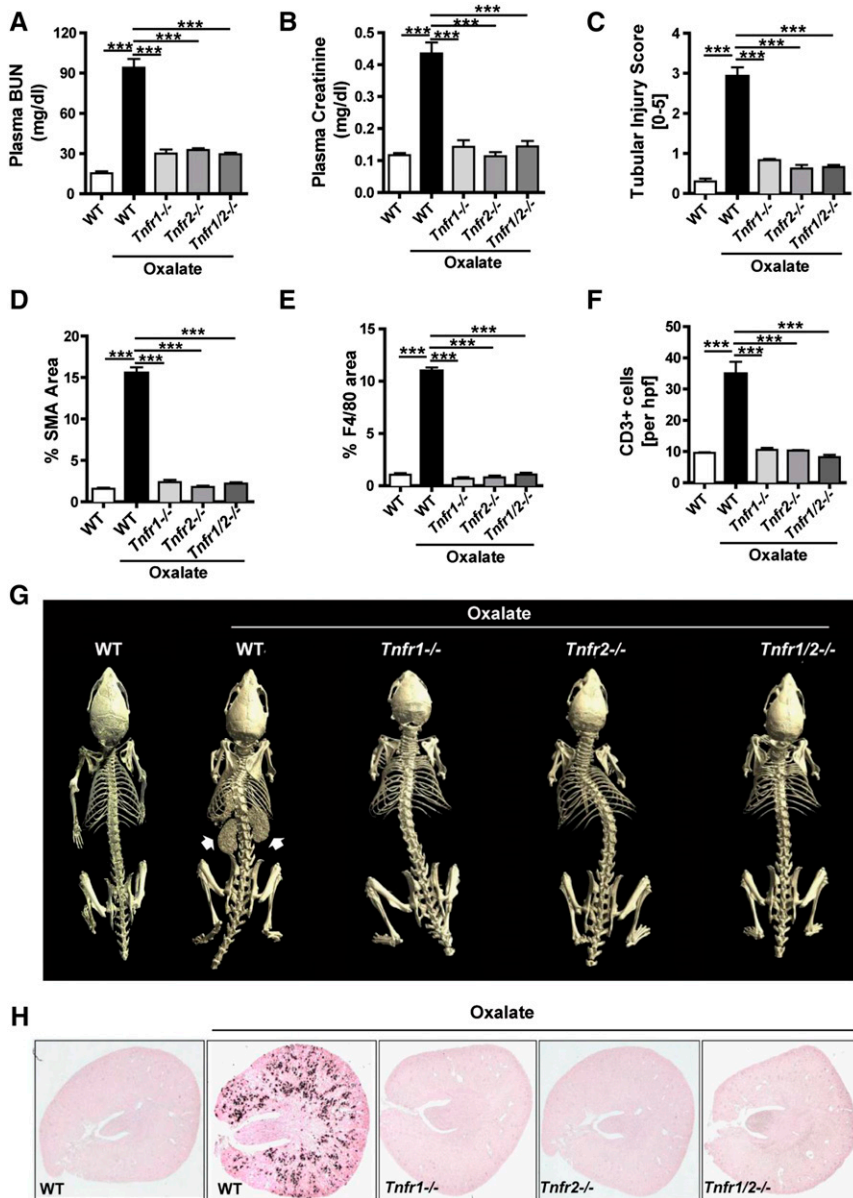
Figure 2. *Tnfr1*-, *Tnfr2*-, and *Tnfr1/2*-deficient mice are protected from hyperoxaluria-related CKD and nephrocalcinosis. C57BL/6 wild type and *Tnfr1*-, *Tnfr2*-, and *Tnfr1/2*-deficient mice were fed either high oxalate or control diet for 14 days. (A) Plasma BUN and (B) plasma creatinine were measured. (C–F) Quantification of (C) tubular injury, (D) SMA+ area, (E) F4/80+ staining for macrophages, and (F) CD3+ cells per high power field. (G) Diagnostic imaging was performed using computed tomography. Arrows indicate the kidneys filled with CaOx crystals. (H) Pizzolato staining of kidney sections. Note that kidneys of wild-type mice, but not *Tnfr1*-, *Tnfr2*-, and *Tnfr1/2*-deficient mice fed with a high oxalate diet show CaOx monohydrate crystal deposition. Original magnification ×25. Data are means±SEM from six to seven mice in each group. ***P<0.001.

inhibition of TNFR signaling has protective effects on nephrocalcinosis and CKD in hyperoxaluria. With an oxalate-rich diet, *Tnfr1*-, *Tnfr2*-, and *Tnfr1/2*-deficient mice displayed a complete absence of intrarenal CaOx deposits; although they developed the same degree of hyperoxaluria and had same levels of calcium in urine as their wild-type counterparts of the same genetic background that developed progressive nephrocalcinosis and CKD.

Computed tomography, Pizzolato staining, and urinary mineral analysis consistently documented these findings in each genotype. This finding first came as a surprise and prompted us to consider direct crystal receptor interactions, as has been reported for uric acid crystals and C-type lectin family 12, member A,[24] or cholesterol crystals and human macrophage-inducible C-type lectin.[25] However, TNFR1-IgG and TNFR2-IgG fusion proteins did not bind to CaOx crystals.

Having excluded this option, we considered intrinsic TNFR ligands to induce TNFR signaling-related crystal adhesion. Several groups have presented convincing experimental data that hyperoxaluria-related nephrocalcinosis depends on the expression of several molecules on the luminal surface of tubular epithelial cells that promote crystal adhesion and intrarenal crystal plug formation.[7–14] We focused on CD44 and annexin II, for which consistent data have been published.[26] Several lines of evidence support a role of TNFRs in inducing surface expression of these molecules in tubular epithelial cells. We demonstrate that CaOx crystals induced their mRNA expression in tubular cells isolated from wild-type but not *Tnfr*-deficient mice. The same phenomenon was observed in hyperoxaluric mice at mRNA and protein level *in vivo*. Although not ultimately proven by reconstitution experiments, it seems likely that the prevention of intrarenal crystal adhesion molecule expression explains the lack of nephrocalcinosis in the TNFR-mutant mouse strains. Given the lack of nephrocalcinosis and kidney injury, a putative role for the TNFRs in nephrocalcinosis-related intrarenal inflammation and CKD progression remains speculative and could not be studied. Also, the possibility of differential renal oxalate handling in the TNFR-mutant mouse strains cannot be completely ignored. However, the nonredundant role of TNFR1 and TNFR2 for hyperoxaluria-induced nephrocalcinosis created the rationale for considering TNFR signaling as a therapeutic target in chronic oxalate nephropathy.
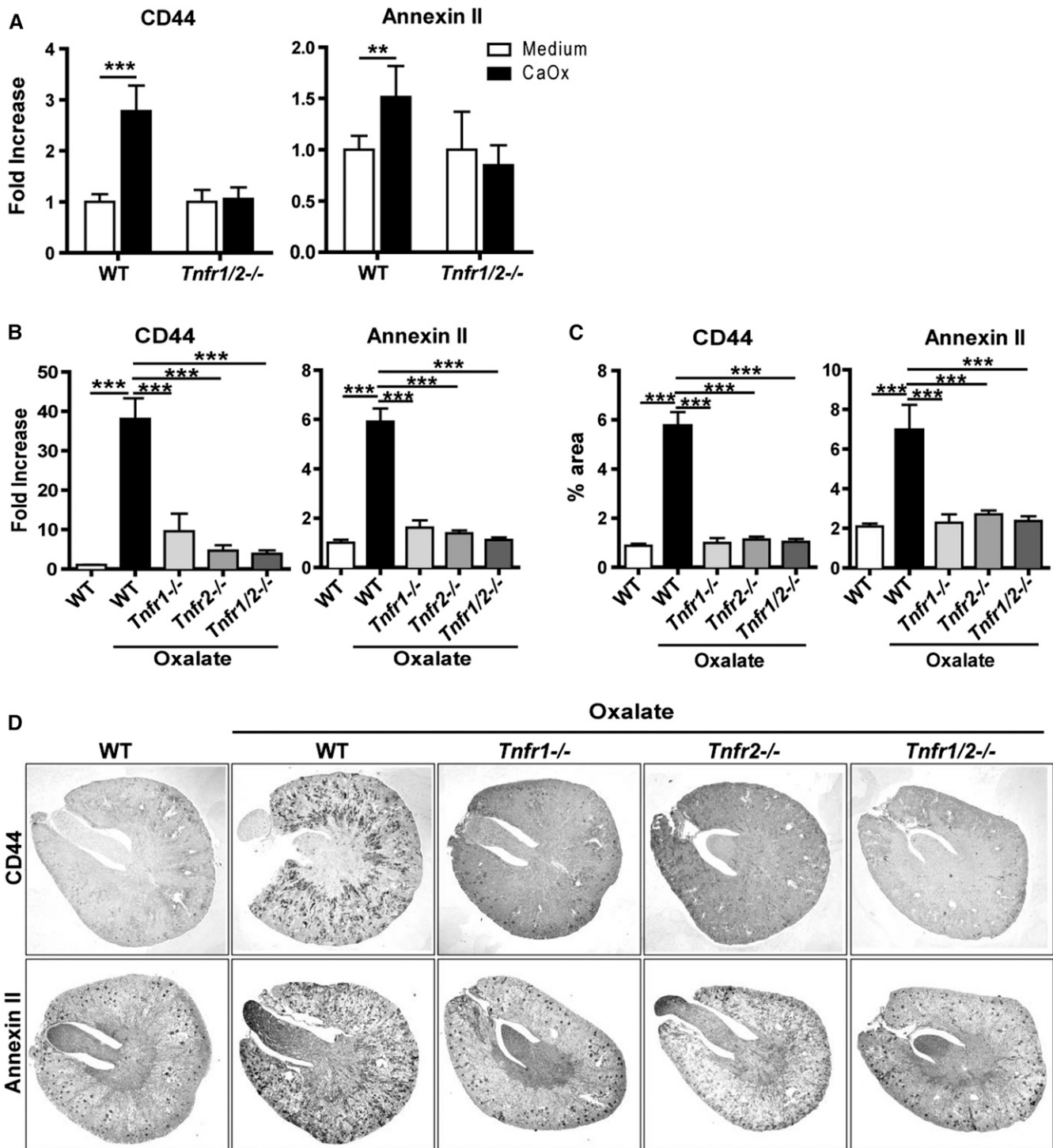
Figure 3. TNFRs are required to mediate CaOx crystal adhesion to tubular cells. (A) Primary isolated tubular epithelial cells from C57BL/6 and *Tnfr1/2*-deficient mice were stimulated with 300 μg/ml of CaOx monohydrate (CaOx) crystals for 6 hours and the gene expression for CD44 and annexin II were analyzed. Data are mean±SEM from three independent experiments. (B–D) C57BL/6 wild type and *Tnfr1*-, *Tnfr2*-, and *Tnfr1/2*-deficient mice were fed either high oxalate or control diet for 14 days. (B) Gene expression, (C) quantification, and (D) immunostaining for CD44 and annexin II in kidney tissue. Original magnification ×25. Data are mean±SEM from six to seven mice in each group. **$P<0.01$; ***$P<0.001$.

R-7050 is a small molecule that inhibits the internalization-dependent signaling of TNFR1 and TNFR2.[27–29]

Preemptive R-7050 therapy partially protected wild-type mice from hyperoxaluria-induced nephrocalcinosis

and CKD. The incomplete protection may be related either to other crystal adhesion molecules that are not under the
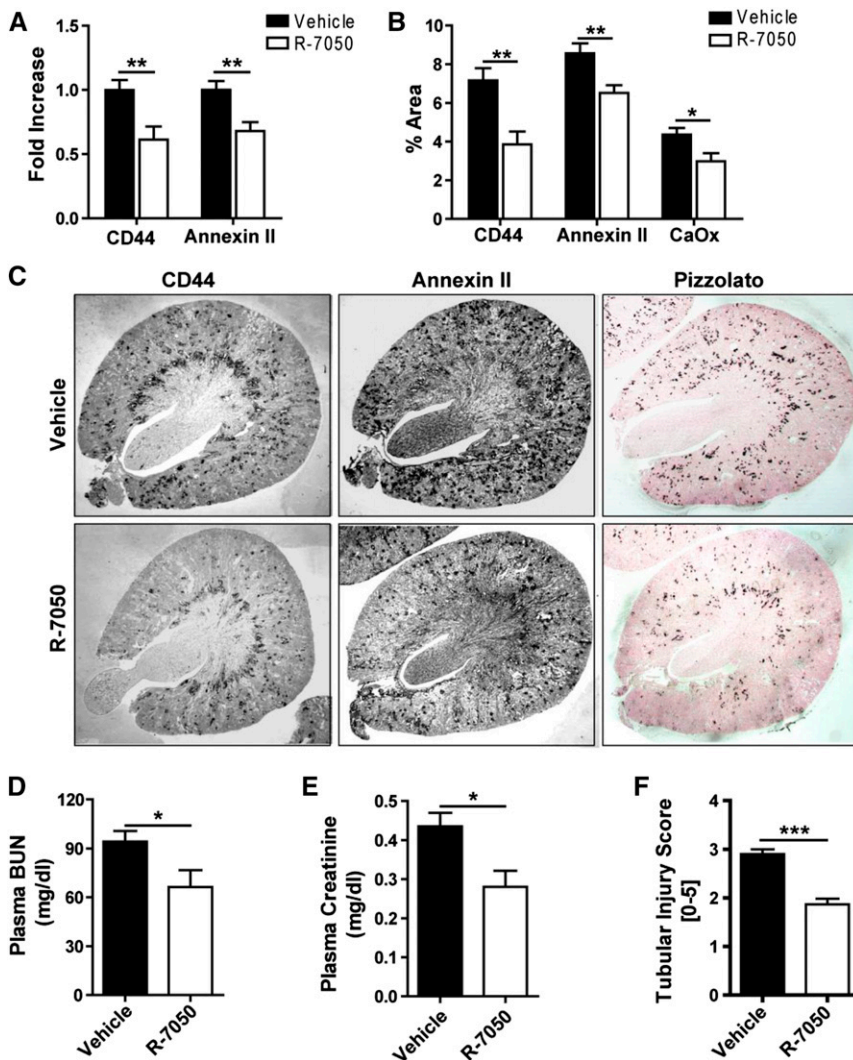
Figure 4. The TNFR antagonist R-7050 protects hyperoxaluric mice from nephrocalcinosis and subsequent CKD. C57BL/6 male mice were fed high oxalate diet for 14 days with or without R-7050 (12 mg/kg intraperitoneally, every alternate day) treatment. (A) Gene expression was analyzed for CD44 and annexin II. (B) Quantification and (C) immunostaining for CD44, annexin II, and Pizzolato staining for CaOx. Original magnification ×25. (D) Plasma BUN and (E) plasma creatinine were measured. (F) Quantification of tubular injury. Data are means±SEM from six to eight mice in each group. *$P<0.05$; **$P<0.01$ versus vehicle group.

control of TNFRs or to dosing and pharmacodynamics of R-7050, but the effects noted were consistent across all end points studied. Initiating treatment after nephrocalcinosis has developed is less likely to be effective, so we would consider initiating TNFR blockade as early as possible in patients with severe hyperoxaluria, to block crystal adhesion from early on.

In summary, TNFR signaling is essential for CaOx crystal adhesion to the luminal membrane of renal tubules, which is a fundamental mechanism for the initiation of nephrocalcinosis. TNFR blockade might be an innovative therapeutic option to delay progressive forms of nephrocalcinosis, *e.g.,* in primary hyperoxaluria.

CONCISE METHODS

Animal Studies
C57BL/6J mice were purchased from Charles River Laboratories (Sulzfeld, Germany). *Tnfr1-* and *Tnfr2-*deficient mice were originally obtained from the Jackson Laboratories

(Bar Harbor, ME) and bred under specific pathogen-free conditions. *Tnfr1/2* double-deficient mice were generated by crossbreeding *Tnfr1-* and *Tnfr2-*deficient mice. Mice were housed in groups of five in filter top cages, with unlimited access to food and water. Cages, nest lets, food, and water were sterilized by autoclaving before use. Male mice aged 6–8 weeks old were used for experiments. Oxalate diet was prepared by adding 50 μmol/g sodium oxalate to a calcium-free standard diet (Ssniff, Soest, Germany) as previously described.[19,22] For intervention studies, C57BL/6 male mice were divided into two groups ($n=9$–10). Each group received either intraperitoneal vehicle (50% dimethyl sulfoxide) or R-7050 (12 mg/kg) every alternate day. Mice were euthanized at day 14 after starting the oxalate diet. Plasma and urine samples were collected at different time points before death by cervical dislocation and were acidified immediately for oxalate estimations. Kidneys were kept at $-80°$C for protein isolation and in RNA later solution at $-20°$C for RNA isolation. One part of the kidney was also kept in formalin to be embedded in paraffin for histologic analysis. All experimental procedures were approved by the local government authorities.

Assessment of Renal Injury
Kidney sections of 2 μm were stained with periodic acid–Schiff reagent, and the tubular injury was scored by assessing the percentage of necrotic tubules and presence of tubular casts. Pizzolato staining was used to visualize CaOx crystals and crystal deposit formation in the kidney was evaluated as described.[22] F4/80+ macrophages and CD3+ T cells (both from Serotec, Oxford, UK) were identified by immunostaining. F4/80+ macrophages were analyzed by assessing the positively stained area in 15 high power fields per section using ImageJ software, whereas CD3+ T cells were counted in 15 high power fields per section. Fibrotic areas were identified by immunostaining for smooth muscle actin (Dako GmbH, Hamburg, Germany) and Masson Trichrome. The expression of crystal adhesion molecules *e.g.,* CD44 and Annexin II was identified by immunostaining for CD44 and Annexin II (both from Abcam, Inc., Cambridge, MA). Quantification of the immunostaining was done using ImageJ software. All assessments were performed by

an observer blinded to the experimental condition. Plasma BUN and creatinine levels were measured using Cobas Integra 800 autoanalyzer (Roche, Basel, Switzerland).

Ultrasound and Microcomputed Tomography

For ultrasound, mice were anesthetized and then images of kidneys were taken using the LOG1QS8 machine, probe L818i (GE healthcare, Waukesha, WI). For the skeletal and renal analysis, datasets were acquired at 9 μm voxel resolution using a SkyScan 1176 *in-vivo* micro-CT (Bruker SkyScan, Kontich, Belgium). Image reconstruction was performed using InstaRecon (InstaRecon, Inc., Urbana, IL) and visualization was done with CTVox (Bruker SkyScan).

x-Ray Diffraction

The analysis of the mouse kidneys by x-ray powder diffraction was performed with the Agilent Super-Nova A S2 (Dual) diffractometer with Atlas S2 detector using the Mova (Mo) x-ray source ($\lambda = 0.71073$ Å). A part of the pulverized kidneys was applied on a Cryo-Loop with perfluorinated oil and x-rayed at a temperature of T = 100 K. Further analysis was done with the Nova (Cu) x-ray source ($\lambda = 1.54184$ Å), where a higher intensity but also a lower signal resolution was noticed. In principle, the results with copper are very similar to those with molybdenum.

Cell Culture Studies

Primary tubular epithelial cells were isolated from kidneys and were maintained in DMEM/F12 containing 10% FCS, 1% penicillin–streptomycin, 125 ng/ml prostaglandin E1 (Calbiochem, San Diego, CA), 25 ng/ml EGF, 1.8 μg/ml l-thyroxine, 3.38 ng/ml hydrocortisone, and 2.5 mg/ml of insulin-transferrin-sodium selenite supplement (all from Sigma-Aldrich, St. Louis, MO). All cells were cultured in an incubator at 37°C, with 5% CO_2, and stimulated with crystals of CaOx (1–2 μm size) (Alfa Aesar, Karlsruhe, Germany).

RNA Preparation and Real-Time Quantitative RT-PCR

Total RNA was isolated from kidneys and *in vitro* cells using a Qiagen RNA extraction kit (Germantown, MD) following the manufacturer's instructions. After quantification, RNA quality was assessed using agarose gels. From isolated RNA, cDNA was prepared using reverse transcription (Superscript II) (Invitrogen, Carlsbad, CA). Real-time RT-PCR was performed using SYBRGreen PCR master mix and was analyzed with a Light Cycler 480 (Roche). All gene expression values were normalized using 18S RNA as a housekeeping gene. All primers used for amplification were from Metabion (Martinsried, Germany), and are listed in Table 1.

Protein Isolations and Immunoblots

Proteins from kidney tissues were extracted using lysis buffer. After determination of protein concentrations, 50 μg of the kidney protein was mixed with 4× SDS loading buffer and was denatured at 95°C for 5 minutes, for Western blot analysis. Proteins were then separated by SDS-PAGE and transferred to a polyvinylidene difluoride membrane. Nonspecific binding to the membrane was blocked for 1 hour at room temperature with 5% nonfat milk in the tris-buffered saline buffer. The membranes were then incubated overnight at 4°C with primary antibodies for TNFR1, TNFR2 (both from Abcam), and β-actin (Cell Signaling Technology, Danvers, MA), followed by incubation with secondary anti-rabbit IgG labeled with HRP. Immunostained bands were detected using a chemiluminescence kit (ECL kit, GE Healthcare), and were further analyzed by densitometry.

Human Samples

Cortical and papillary renal tissue sections were studied from four patients with genetically proven primary hyperoxaluria type 1, as well as one control individual. Kidneys from the four primary hyperoxaluria type 1 patients with ESRD were obtained by native nephrectomy at the time of renal transplant and the clinical characteristics of each of these patients are described in our previous paper (patients 1, 2, 4, and 5, respectively).[30] Cortical and papillary renal tissue was obtained from the kidney of a nonstone former (71 years of age) who underwent a nephrectomy for renal cancer. The work was approved by the Institutional Review Board at both the Mayo Clinic (nos. 11–001702, 11–005413, and 07–008751) and Indiana University (no. 98–073). All papillary and cortical specimens were fixed by immersion in 5% paraformaldehyde in 0.1 mol/L phosphate buffer at pH 7.4, and routinely processed before embedment in a 50:50 mixture of Paraplast Xtra and Pell-away Micro-Cut. Four-micron sections were cut and mounted on glass slides for immunostaining.

Table 1. Primer sequences for RT-PCR

Target	Primer Sequence
KIM-1	Forward 5′-TCAGCTCGGGAATGCACAA -3′
	Reverse 5′-TGGTTGCCTTCCGTGTCTCT -3′
TIMP-2	Forward 5'-CAGACGTAGTGATCAGAGCCAAA -3'
	Reverse 5'-ACTCGATGTCTTTGTCAGGTCC -3'
CCL-5	Forward 5′- GTGCCCACGTCAAGGAGTAT-3′
	Reverse 5′- CCACTTCTTCTCTGGGTTGG-3′
IL-6	Forward 5′- TGATGCACTTGCAGAAAACA -3′
	Reverse 5′- ACCAGAGGAAATTTTCAATAGGC - 3′
Fibronectin	Forward 5′-GGAGTGGCACTGTCAACCTC - 3′
	Reverse 5′-ACTGGATGGGGTGGGAAT - 3′
Collagen1α1	Forward 5′-ACATGTTCAGCTTTGTGGACC -3′
	Reverse 5′-TAGGCCATTGTGTATGCAGC- 3′
FSP-1	Forward 5′- CAGCACTTCCTCTCTCTTGG -3′
	Reverse 5′-TTTGTGGAAGGTGGACACAA - 3′
CD44	Forward 5′-AGCGGCAGGTTACATTCAAA-3′
	Reverse 5′-CAAGTTTTGGTGGCACACAG-3′
Annexin II	Forward 5′-GCACATTGCTGCGGTTTGTCAG-3′
	Reverse 5′-CACCAACTTCGATGCTGAGAGG-3′
TNFR1	Forward 5′-GCAACAGCACCGCAGTAGCTGA-3′
	Reverse 5′- GTGCGTCCCTTGCAGCCACT-3′
TNFR2	Forward 5′-CTGGGTCGCGCTGGTCTTGC-3′
	Reverse 5′-CAAGACAACCTGGGCGGGCA-3′
18S RNA	Forward 5′- GCAATTATTCCCCATGAACG-3′
	Reverse 5′- AGGGCCTCACTAAACCATCC- 3′

Statistical Analyses

Data are presented as mean±SEM. A comparison of groups was performed using ANOVA, and *post hoc* Bonferroni correction was used for multiple comparisons. A value of $P<0.05$ was considered to indicate statistical significance.

DISCLOSURES

None.

REFERENCES

1. Worcester EM, Coe FL: Clinical practice. Calcium kidney stones. *N Engl J Med* 363: 954–963, 2010
2. Hoppe B: An update on primary hyperoxaluria. *Nat Rev Nephrol* 8: 467–475, 2012
3. Evan AP, Lingeman JE, Coe FL, Parks JH, Bledsoe SB, Shao Y, Sommer AJ, Paterson RF, Kuo RL, Grynpas M: Randall's plaque of patients with nephrolithiasis begins in basement membranes of thin loops of Henle. *J Clin Invest* 111: 607–616, 2003
4. Bhasin B, Ürekli HM, Atta MG: Primary and secondary hyperoxaluria: Understanding the enigma. *World J Nephrol* 4: 235–244, 2015
5. Aggarwal KP, Narula S, Kakkar M, Tandon C: Nephrolithiasis: molecular mechanism of renal stone formation and the critical role played by modulators. *BioMed Res Int* 2013: 292953, 2013
6. Baumann JM, Affolter B: From crystalluria to kidney stones, some physicochemical aspects of calcium nephrolithiasis. *World J Nephrol* 3: 256–267, 2014
7. Asselman M, Verhulst A, De Broe ME, Verkoelen CF: Calcium oxalate crystal adherence to hyaluronan-, osteopontin-, and CD44-expressing injured/regenerating tubular epithelial cells in rat kidneys. *J Am Soc Nephrol* 14: 3155–3166, 2003
8. Wesson JA, Ward MD: Role of crystal surface adhesion in kidney stone disease. *Curr Opin Nephrol Hypertens* 15: 386–393, 2006
9. Sheng X, Jung T, Wesson JA, Ward MD: Adhesion at calcium oxalate crystal surfaces and the effect of urinary constituents. *Proc Natl Acad Sci U S A* 102: 267–272, 2005
10. Lieske JC, Swift H, Martin T, Patterson B, Toback FG: Renal epithelial cells rapidly bind and internalize calcium oxalate monohydrate crystals. *Proc Natl Acad Sci U S A* 91: 6987–6991, 1994
11. Sheng X, Ward MD, Wesson JA: Adhesion between molecules and calcium oxalate crystals: critical interactions in kidney stone formation. *J Am Chem Soc* 125: 2854–2855, 2003
12. Sheng X, Ward MD, Wesson JA: Crystal surface adhesion explains the pathological activity of calcium oxalate hydrates in kidney stone formation. *J Am Soc Nephrol* 16: 1904–1908, 2005
13. Verhulst A, Asselman M, Persy VP, Schepers MS, Helbert MF, Verkoelen CF, De Broe ME: Crystal retention capacity of cells in the human nephron: involvement of CD44 and its ligands hyaluronic acid and osteopontin in the transition of a crystal binding- into a nonadherent epithelium. *J Am Soc Nephrol* 14: 107–115, 2003
14. Kumar V, Farell G, Deganello S, Lieske JC: Annexin II is present on renal epithelial cells and binds calcium oxalate monohydrate crystals. *J Am Soc Nephrol* 14: 289–297, 2003
15. Cochat P, Rumsby G: Primary hyperoxaluria. *N Engl J Med* 369: 649–658, 2013
16. Mulay SR, Anders HJ: Crystallopathies. *N Engl J Med* 374: 2465–2476, 2016
17. Nazzal, L, Puri, S, Goldfarb, DS: Enteric hyperoxaluria: an important cause of end-stage kidney disease. *Nephrol Dial Transplant* 31: 375–382, 2015
18. Mulay SR, Kulkarni OP, Rupanagudi KV, Migliorini A, Darisipudi MN, Vilaysane A, Muruve D, Shi Y, Munro F, Liapis H, Anders HJ: Calcium oxalate crystals induce renal inflammation by NLRP3-mediated IL-1β secretion. *J Clin Invest* 123: 236–246, 2013
19. Knauf F, Asplin JR, Granja I, Schmidt IM, Moeckel GW, David RJ, Flavell RA, Aronson PS: NALP3-mediated inflammation is a principal cause of progressive renal failure in oxalate nephropathy. *Kidney Int* 84: 895–901, 2013
20. Mulay SR, Desai J, Kumar SV, Eberhard JN, Thomasova D, Romoli S, Grigorescu M, Kulkarni OP, Popper B, Vielhauer V, Zuchtriegel G, Reichel C, Bräsen JH, Romagnani P, Bilyy R, Munoz LE, Herrmann M, Liapis H, Krautwald S, Linkermann A, Anders HJ: Cytotoxicity of crystals involves RIPK3-MLKL-mediated necroptosis. *Nat Commun* 7: 10274, 2016
21. Evan AP, Coe FL, Gillen D, Lingeman JE, Bledsoe S, Worcester EM: Renal intratubular crystals and hyaluronan staining occur in stone formers with bypass surgery but not with idiopathic calcium oxalate stones. *Anat Rec (Hoboken)* 291: 325–334, 2008
22. Mulay, SR, Eberhard, JN, Pfann, V, Marschner, JA, Darisipudi, MN, Daniel, C, Romoli, S, Desai, J, Grigorescu, M, Kumar, SV, Rathkolb, B, Wolf, E, Hrabe de Angelis, M, Bauerle, T, Dietel, B, Wagner, CA, Amann, K, Eckardt, KU, Aronson, PS, Anders, HJ, Knauf, F: Oxalate-induced chronic kidney disease with its uremic and cardiovascular complications in C57BL/6 mice. *Am J Physiol Renal Physiol* 310: F785–F795, 2016
23. Mulay SR, Evan A, Anders HJ: Molecular mechanisms of crystal-related kidney inflammation and injury. Implications for cholesterol embolism, crystalline nephropathies and kidney stone disease. *Nephrol Dial Transplant* 29: 507–514, 2014
24. Neumann K, Castiñeiras-Vilariño M, Höckendorf U, Hannesschläger N, Lemeer S, Kupka D, Meyermann S, Lech M, Anders HJ, Kuster B, Busch DH, Gewies A, Naumann R, Groß O, Ruland J: Clec12a is an inhibitory receptor for uric acid crystals that regulates inflammation in response to cell death. *Immunity* 40: 389–399, 2014
25. Kiyotake R, Oh-Hora M, Ishikawa E, Miyamoto T, Ishibashi T, Yamasaki S: Human Mincle Binds to Cholesterol Crystals and Triggers Innate Immune Responses. *J Biol Chem* 290: 25322–25332, 2015
26. Taguchi K, Okada A, Kitamura H, Yasui T, Naiki T, Hamamoto S, Ando R, Mizuno K, Kawai N, Tozawa K, Asano K, Tanaka M, Miyoshi I, Kohri K: Colony-stimulating factor-1 signaling suppresses renal crystal formation. *J Am Soc Nephrol* 25: 1680–1697, 2014
27. King MD, Alleyne CH Jr, Dhandapani KM: TNF-alpha receptor antagonist, R-7050, improves neurological outcomes following intracerebral hemorrhage in mice. *Neurosci Lett* 542: 92–96, 2013
28. Wu W, Zhang H: Role of tumor necrosis factor-α and interleukin-1β in anorexia induction following oral exposure to the trichothecene deoxynivalenol (vomitoxin) in the mouse. *J Toxicol Sci* 39: 875–886, 2014
29. Ma Y, Cheng Q, Wang E, Li L, Zhang X: Inhibiting tumor necrosis factor-α signaling attenuates postoperative cognitive dysfunction in aged rats. *Mol Med Rep* 12: 3095–3100, 2015
30. Worcester EM, Evan AP, Coe FL, Lingeman JE, Krambeck A, Sommers A, Phillips CL, Milliner D: A test of the hypothesis that oxalate secretion produces proximal tubule crystallization in primary hyperoxaluria type I. *Am J Physiol Renal Physiol* 305: F1574–F1584, 2013

This article contains supplemental material online at http://jasn.asnjournals.org/lookup/suppl/doi:10.1681/ASN.2016040486/-/DCSupplemental.